Dyes and Pigments 98 (2013) 190–194

Contents lists available at SciVerse ScienceDirect

Dyes and Pigments

journal homepage: www.elsevier.com/locate/dyepig

A pyrene-phenanthroimidazole derivative for non-doped blue organic light-emitting devices

Ying Zhang [a,b], Tsz-Wai Ng [b], Feng Lu [a], Qing-Xiao Tong [a,**], Shiu-Lun Lai [c], Mei-Yee Chan [c], Hoi-Lun Kwong [d], Chun-Sing Lee [b,*]

[a] Department of Chemistry, Shantou University, Guangdong 515063, China
[b] Center of Super-Diamond and Advanced Films (COSDAF) and Department of Physics and Materials Science, City University of Hong Kong, Hong Kong, China
[c] Department of Chemistry, University of Hong Kong, Hong Kong, China
[d] Department of Biology and Chemistry, City University of Hong Kong, Hong Kong, China

ARTICLE INFO

Article history:
Received 1 August 2012
Received in revised form
29 January 2013
Accepted 30 January 2013
Available online 4 March 2013

Keywords:
Non-doped
Blue emitter
Pyrene-based
OLED
Dual function
Hole transporter

ABSTRACT

We report a newly synthesized blue fluorescent pyrene-phenanthroimidazole based emitter **Py-BPI** and its applications in non-doped organic light-emitting devices (OLEDs). **Py-BPI** has a high fluorescence quantum yield of 40% and good thermal stability with a high glass transition temperature of 137 °C. Based on **Py-BPI**, OLEDs with several configurations have been fabricated. Among these devices, an OLED with only two organic layers of **Py-BPI** and BPhen demonstrates blue emission with high efficiencies of 3.93 cd/A and 3.2 lm/W and maintains a high efficiency of 3.83 cd/A even at a brightness of 5000 cd/m^2. Combining with its hole-transporting ability, **Py-BPI** is shown to be a versatile blue emitter especially suitable for high brightness applications.

1. Introduction

Blue organic light-emitting devices (OLEDs) have been extensively researched for their applications in full-color displays and solid-state lighting. However, performance of blue emitters is still lagging behind those of red and green materials [1,2]. Development of high performance blue emitters is thus an important task. Common blue fluorescent molecules can be roughly classified into several groups according to their emitting cores including anthracene, fluorene, pyrene etc. Among these, pyrene derivatives have rich electronic and photophysical properties and usually have good carriers mobilities stem from their large π-conjugated systems [3–5]. Many high efficiency organic materials conjugated with pyrene unit have been reported in the past few years [6–9]. However, there are few high efficiency blue light-emitting materials based on pyrene derivatives owing to their large conjugation and strong tendency to form excimers, which causes red-shifted emissions as well as decrease in the fluorescence efficiency in solid-state [10].

On the other hand, complicated multilayer device structures are not preferred for large-scale industrial processing. Devices with fewer layers are thus more favorable for simplifying the fabrication process. Development of multifunctional materials, which can be used both for carrier transport and light-emission, is thus highly desirable [10]. By linking phenanthroimidazole with pyrene via a thiophene bridge, we have obtained a yellowish green emitter **Py-TPI**(Scheme 1) [11]. In this work, we explore the effects of changing the thiophene bridge to a benzene bridge and obtained a new blue emitter – **Py-BPI**. With this simple change, emission from the corresponding OLED shows a sharp blue-shift, a significant change in CIE coordinates from (0.32, 0.59) to (0.15, 0.18) as well as enhanced device efficiency. **Py-BPI** also has a shallow highest occupied molecular orbital (HOMO) energy level of 5.4 eV which facilitates efficient hole-injection. In addition, it is also shown that **Py-BPI** is capable to function as both a blue emitter and a hole-transporter in OLED.

* Corresponding author.
** Corresponding author.
E-mail addresses: qxtong@stu.edu.cn (Q.-X. Tong), apcslee@cityu.edu.hk (C.-S. Lee).

0143-7208/$ – see front matter © 2013 Elsevier Ltd. All rights reserved.
http://dx.doi.org/10.1016/j.dyepig.2013.01.022

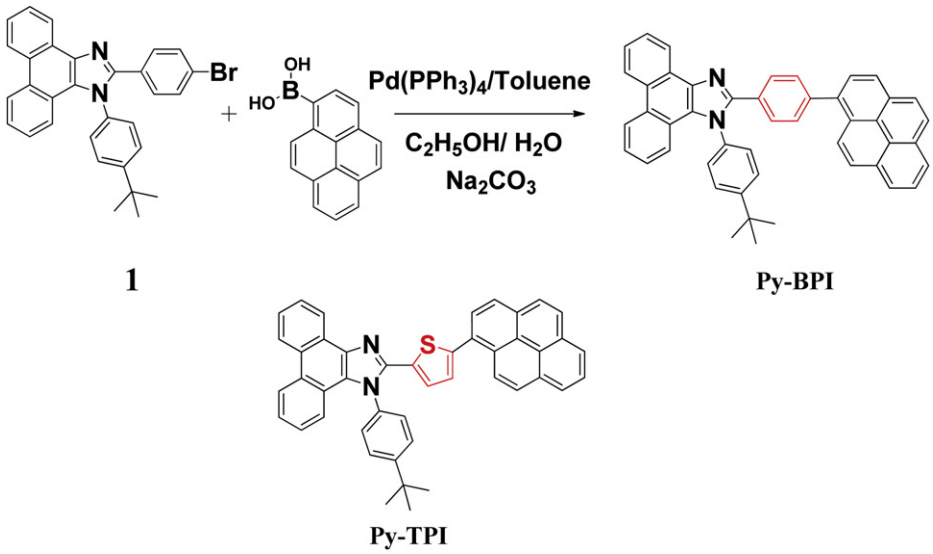

Scheme 1. A synthetic route for **Py-BPI** and the chemical structure of Py-TPI.

2. Experimental

2.1. Organic synthesis

All solvents and materials were used as received from commercial suppliers without further purification. A synthetic route of the product 1-(4-tert-butylphenyl)-2-(4-(pyren-1-yl)phenyl)-1H-phenanthro [9, 10-d] imidazole (**Py-BPI**)is outlined in Scheme 1. In particular, 2-(4-Bromophenyl)-1-(4-tert-butylphenyl)-1H-phenanthro [9, 10-d] imidazole was prepared according to the procedures described in our previous work [12] and **Py-BPI** was synthesized via a Suzuki coupling reaction [13].

2.1.1. 1-(4-tert-butylphenyl)-2-(4-(pyren-1-yl)phenyl)-1H-phenanthro [9,10-d] imidazole(Py-BPI)

The synthesis procedure is similar to that reported in our previous work [12]. ^{1}H NMR (400 MHz, CD_2Cl_2) δ1.50 (s, 9H), 7.28–7.37 (m, 2H), 7.52–7.66 (m, 5H), 7.67–7.87 (m, 6H), 8.01–8.10 (m, 3H), 8.12–8.30 (m, 6H), 8.75–8.91 (m, 3H).^{13}C NMR(75 MHz, $CDCl_3$) δ31.64 (s), 35.37 (s), 121.26 (s), 123.32 (s), 123.71 (s), 124.39 (s), 124.74–125.41 (m), 125.47 (s), 126.30 (s), 126.72 (s), 127.22–127.57 (m), 127.57–128.85 (m), 128.86 (s), 130.32 (d), 131.08 (d), 131.65 (s). TOF MS (EI+): 626.2777.Calc. for $C_{47}H_{34}N_2$: 626.27.Anal. Found: C, 89.11; H, 6.34; N, 4.33. Calc. for $C_{47}H_{34}N_2$: C, 90.06; H, 5.47; N, 4.47.

2.2. Material characterization

Nuclear magnetic resonance (NMR) spectrum was recorded using CD_2Cl_2(^{1}HNMR) and $CDCl_3$(^{13}CNMR) as solvents with a Varian Gemin-400 spectrometer. Mass spectrum was recorded on a PE SCIEX API-MS system. Absorption and photoluminescence (PL) spectra of **Py-BPI** were recorded on a Perkin–Elmer Lambda 2S UV–visible spectrophotometer and a Perkin–Elmer LS50 fluorescence spectrometer, respectively. Fluorescence quantum yields (Φ_f) in dichloromethane solution were determined according to previous literature [14] by a comparative method, using anthracene as a standard reference with $\Phi_f = 0.27$ in ethanol. Thermogravimetric analysis (TGA) was performed on a TA Instrument TGAQ50 at a heating rate of 10 °C/min under a nitrogen atmosphere. Differential scanning calorimetric (DSC) measurement was performed on a TA Instrument DSC2910. The sample was first heated at a rate of 10 °C/min to melt and then quenched. Glass transition temperature (T_g) of **Py-BPI** was determined by heating the quenched sample at a heating rate of 10 °C/min. Ionization potential (I_P) of **Py-BPI** film on ITO glass substrate was measured via ultraviolet photoelectron spectroscopy (UPS) in a VG ESCALAB 220i-XL surface analysis system. Electron affinity (E_A) of **Py-BPI** was estimated by subtracting from I_P with its optical band gap (E_{gap}) determined from the absorption spectra of its solid-state film.

2.3. OLED fabrication

Patterned indium-tin oxide (ITO) coated glass slides with a sheet resistance of 30 Ω per square were sequentially cleaned with isopropyl alcohol, Decon 90, rinsed in de-ionized water, then dried in an oven, and finally treated in an ultraviolet-ozone chamber. The ITO substrates were then transferred into a deposition chamber with a base pressure of 10^{-6} mbar. Trilayer and bilayer devices with configurations respectively of ITO/NPB (60 nm)/**Py-BPI** (40 nm)/electron transporting layer(20 nm)/LiF (0.5 nm)/Mg: Ag (100 nm) and ITO/Py-BPI (100 nm)/ETL (20 nm)/LiF (0.5 nm)/Mg:Ag (100 nm)were fabricated by thermal vapor deposition.In these devices either TPBI(1,3,5-Tris(1-phenyl-1H-benzimidazol-2-yl)benzene) or BPhen (4,7-diphenyl-1,10-phenanthroline) was used as an electron-transporting layer (ETL); **Py-BPI** was used as the emitting layer (EML). NPB (4,4′-bis[N-(1-naphthyl)-N-phenylamino] biphenyl) and **Py-BPI** was respectively used as a hole-transporting layer (HTL) in the trilayer and bilayer devices. Deposition rates for both organic and metal layers were monitored with a quartz oscillation crystal and controlled in the range from 1 to 2 Å/s. A shadow mask was used to define the cathode to make four devices each with an active area of 0.1 cm^2. Electroluminescence (EL) spectra, CIE coordinates, and current density–voltage-luminance (J-V-L) characteristics of OLEDs were measured with a programmable Keithley model 237 power source and Spectrascan PR 650photospectrometer under ambient conditions without sample encapsulation.

3. Results and discussion

The synthetic route for **Py-BPI** and its chemical structure are shown in Scheme 1. **Py-BPI** was prepared via Suzuki coupling reactions between 2-(4-Bromophenyl)-1-(4-tert-butylphenyl)-1H-

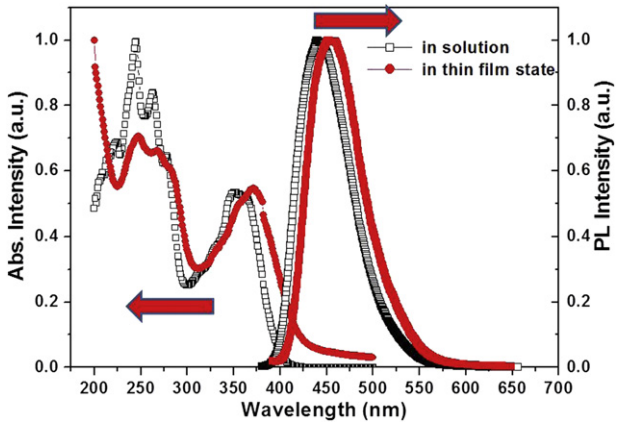

Fig. 1. UV–Vis absorption and photo-luminescence (PL) for **Py-BPI** in dichloromethane solution and thin solid film state.

Table 1
Photophysical and thermal data of Py-BPI and Py-TPI (For comparison purpose, data for Py-TPI are extracted from Ref. [11]).

Compound	Abs (nm)	PL (nm)	Φ_f	T_d (°C)	T_g (°C)	T_m (°C)
Py-BPI	242,262,352[a]/247, 271,371[b]	439[a]/451[b]	40%	431	137	300
Py-TPI	243,343,381[a]/243, 406[b]	485[a]/504, 521[b]	23%	422	128	249

[a] Obtained from dichloromethane solution.
[b] Obtained from thin film state.

phenanthro [9, 10-d] imidazole and pyrenyl-1-boronic acid with a yield of 58%. The molecular structure of **Py-BPI** was confirmed with H nuclear magnetic resonance and mass spectrometry (details shown in Fig. S1 and S2). Attached with a large and rigid pyrene group, **Py-BPI** has good thermal stability with a high decomposition temperature (T_d) of431 °C in nitrogen, a high melting temperature (T_m) up to 300 °C and a glass-transition temperature (T_g) of 137 °C (Fig. S3 and S4).

UV–Vis absorption and PL spectra of **Py-BPI** in both dichloromethane solution and solid-state thin film formed on quartz substrate are shown in Fig. 1.Similarity of the solution and the solid film spectra suggest that intermolecular interaction of **Py-BPI** in solid is weak. Intensive blue emission peaked at wavelength of 451 nm and absorption peaks at 247, 271, and 371 nm in thin-film state were observed. In addition, **Py-BPI** shows a Φ_f of 40%, which is considerably higher than that of **Py-TPI** ($\Phi_f = 23\%$). Such substantial blue-shift of 70 nm over that of the reported **Py-TPI** (i.e.521 nm) and the high Φ_f suggest that they have good potential to offer high efficiency blue emission in OLEDs. The large blue-shift of the PL spectrum of **Py-BPI** compared with **Py-TPI** might be due to the weaker electron donating property of the benzene ring rendering with a deeper HOMO energy level (ie. 5.4 eV) and thus a higher energy gap in **Py-BPI**. Key thermal and photophysical data of the two compounds are summarized in Table 1.

Table 2
Performance data of the OLED based on **Py-BPI**.

Devices	V_{Onset}[a] (V)	V at 20 mA/cm^2 (V)	EL_{max} (nm)	CE^b_{max} (cd/A)	PE^c_{max} (lm/W)	CIE (x, y)
Trilayer-BPhen	2.5	4.0	468	3.27	3.17	0.15,0.18
Trilayer-TPBI	3.0	5.0	468	2.96	2.00	0.15, 0.19
Bilayer-BPhen	3.4	7.6	468	3.93	3.20	0.16, 0.20
Bilayer-TPBI	3.2	5.4	468	2.03	1.00	0.15, 0.15

[a] Obtained at 1 cd/m.^{2}.
[b] Current efficiency of the devices.
[c] Power efficiency of the devices.

It is well known that efficient carrier injection at interfaces between different layers in OLEDs is essential for obtaining high performance devices. It is thus important for the EML to possess a shallow HOMO for facilitating hole-injection [10]. The HOMO value for **Py-BPI** was measured via UPS to be 5.4 eV; while the lowest unoccupied molecular orbital (LUMO) energy is estimated to be 2.7 eV by subtracting the HOMO value with the optical band gap as determined from the absorption cutoff. Schematic energy level diagrams for the **Py-BPI** based OLEDs are shown in Fig. 2.From the diagrams, it can be seen that there are only a small energy step for electron injection (0.2 eV) at the interface of **Py-BPI**/BPhen. In addition, the similar HOMO energies of **Py-BPI** and NPB facilitate efficient hole transport from NPB to **Py-BPI**.

Other than the conventional trilayer devices (ITO/NPB (60 nm)/**Py-BPI** (40 nm)/BPhen or TPBI (20 nm)/LiF (0.5 nm)/Mg:Ag (100 nm)), we also explore the feasibility of using **Py-BPI** as the HTL in bilayer devices (ITO/**Py-BPI** (100 nm)/BPhen or TPBI (20 nm)/LiF (0.5 nm)/Mg:Ag (100 nm)). Key performance data of the four devices were summarized in Table 2.

Fig. 3 shows that electroluminescence (EL) spectra of the four devices are all similar to the PL spectrum of **Py-BPI**. This confirms that the blue emissions of the devices are originated from **Py-BPI**. The EL spectra peak at 468 nm for all four devices with full widths at half maxima range from 82 to 93 nm. Commission Internationale de L'Eclairage (CIE) coordinates of the devices are listed in Table 2. All devices show blue emission with $CIE_y < 0.20$. Comparing with similarly structured trilayer device using **Py-TPI** as the emitter, the CIE coordination moved from (0.32, 0.59) to (0.15, 0.18).

Fig. 4 shows J-V-L characteristics of the four devices based on **Py-BPI**. It can be seen that the driving voltages at the same current

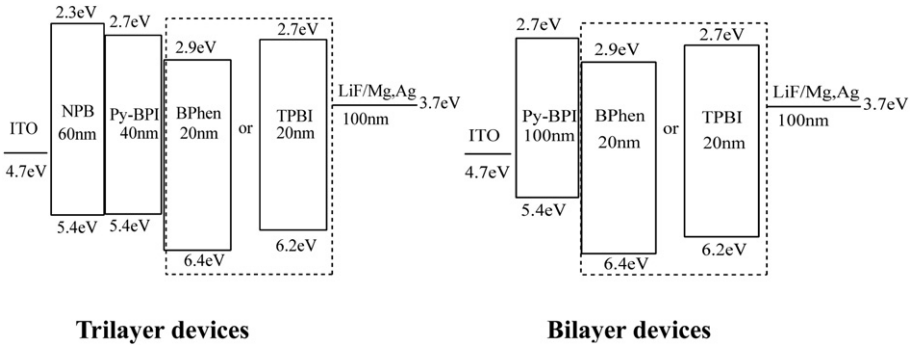

Fig. 2. Schematic energy level diagrams for devices based on **Py-BPI** as an emitter or a dual functional material as both an emitter and a hole transporter.

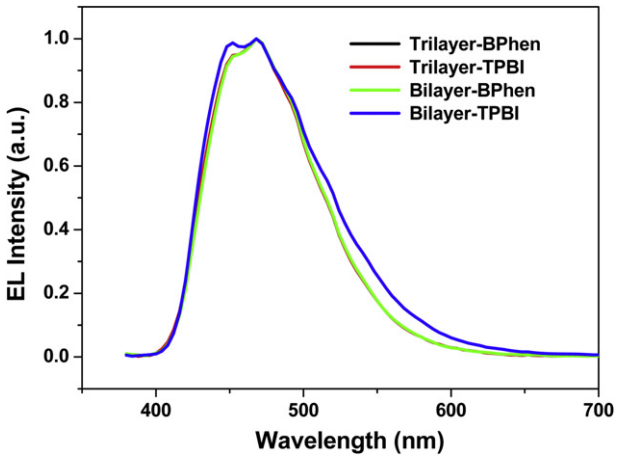

Fig. 3. Electroluminescence (EL) spectra for **Py-BPI** as an emitter in different devices.

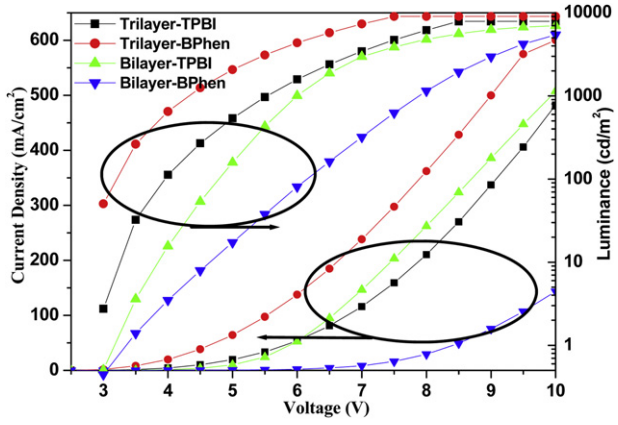

Fig. 4. Current density–voltage and luminance–voltage characteristics of OLEDs based on **Py-BPI**. (To avoid overdriving the devices and/or protection of the measurement system, the maximum brightness was limited to 10000 cd/m^2.)

density or luminance for **Py-BPI** based devices using a BPhen ETL is lower than those of the devices with a TPBI ETL. For instance, at the current density of 20 mA/cm^2 (or at a typical display brightness of 100 cd/m^2), the operating voltage for devices trilayer and bilayer devices with a BPhen ETL are 4.0 and7.6 V (3.2 and 6.2 V) while those using a TPBI ETL are 5.0 and 5.4 V (4.0 and 4.8 V), respectively. In addition, we observed the same trend in the turn-on voltage

Table 3
Summary of device performances for blue OLED with CIEy < 0.20 reported recently.

Emitter	CE (cd/A)	PE (lm/W)	CIE	Ref.
Py-BPI	3.93	3.2	(0.15, 0.20)	This work
TPA-BPI	2.63	2.53	(0.15, 0.09)	[12]
BPyC	2.94	2.72	(0.15, 0.18)	[9]
DPEC	4.75	2.55	(0.15, 0.18)	[8]
Ph3TPE	3.7	2.5	(0.17, 0.20)	[18]
9TPAFSPO	1.5	2.19	(0.16, 0.07)	[19]
BPTF	2.06	–	(0.15, 0.13)	[20]
Silylene-bridged 2-(2-naphthyl) indole	3.8	3.6	(0.15, 0.09)	[21]
TPA-AN	4.54	4.02	(0.15, 0.19)	[22]
MADN	1.43	0.7	(0.15, 0.10)	[23]
TBADN	2.00	–	(0.16, 0.14)	[24]
BDMA	2.20	–	(0.16, 0.12)	[25]
NSA	7.85	–	(0.15, 0.18)	[26]
P2	3.08	1.17	(0.17, 0.19)	[27]
DPF	6.00	3.6	(0.15, 0.19)	[28]
TPIP	4.69	2.71	(0.15, 0.09)	[29]
PhQ-CVz	2.06	1.77	(0.15, 0.09)	[30]
POAn	3.2	3.3	(0.15, 0.07)	[31]
5[a]	2.8	2.33	(0.15, 0.08)	[32]

[a] 9-(4-(10-(Naphthalen-1-yl)anthracen-9-yl)phenyl)-9H-carbazole.

(V_{Onset} is defined as voltage required to give a luminance of 1 cd/m^2):trilayer-BPhen (2.5 V) < trilayer-TPBI (3.0 V); bilayer-BPhen (2.8) < bilayer-TPBI (3.2 V). The reason for the lower driving and onset voltages for the BPhen devices is attributed to the higher electron mobility (μ_e) and deeper LUMO for BPhen as compare to those of TPBI. μ_e under the electric field of 4.9 × 10^5 V/cm from time-of-flight measurement are 5 × 10^{-4} cm^2/V [15] and 3.6 × 10^{-5} cm^2/V [16] for BPhen and TPBI; while LUMO values are 2.9 and 2.7 eV for BPhen and TPBI as we determined. In addition, the incorporation of high hole mobility material NPB (μ_h = 7 × 10^{-3} cm^2/V [17] under the electric field of 4.9 × 10^5 V/cm^2) in trilayer device further reduces the operation voltages.

Fig. 5 shows the power and current efficiencies of the **Py-BPI** based devices under different current densities. The maximum power and current efficiencies for trilayer devices with TPBI are 2.00 lm/W and 2.96 cd/A, respectively whereas those for the trilayer device with BPhen are 3.17 lm/W and 3.27 cd/A, respectively. Interestingly, efficiencies in the bilayer device with BPhen can be further improved to 3.20 lm/W and 3.93 cd/A. Importantly, the current efficiency undergoes negligible change at very high current density of 300 mA/cm^2. It indicates the holes and electrons are well balanced in the bilayer BPhen device. In addition, it is worth noting that performance of **Py-BPI** based devices are comparable to some of the best blue emitters reported recently (Table 3) [8,9,12,18–32].

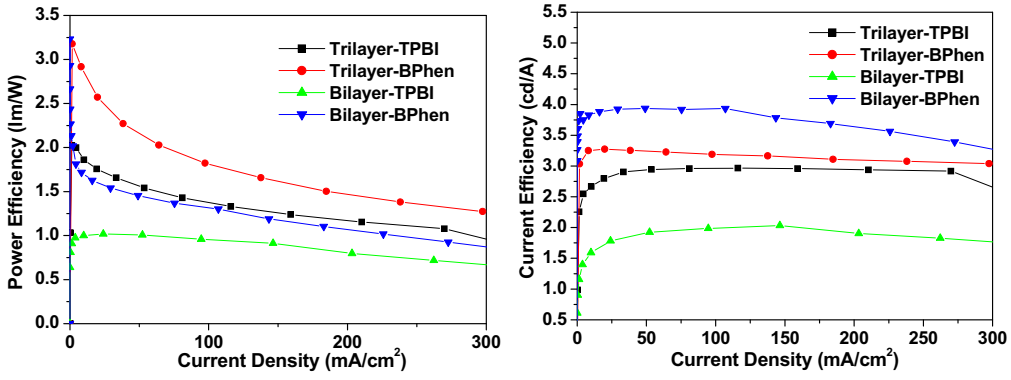

Fig. 5. Power and current efficiencies of the **Py-BPI** based devices under different current densities.

In addition, its additional hole-transporting capability and slow efficiency roll-off at high excitation densities makes it a versatile high performance blue emitter especially suitable for high brightness applications.

4. Conclusion

A newly synthesized blue fluorescence emitter based on pyrene-phenanthroimidazole, namely **Py-BPI**, has been characterized and applied in non-doped OLEDs. **Py-BPI** shows good thermal stability with a T_g of 137 °C and a high Φ_f of 40%. It is found that the PL spectrum of **Py-BPI** was successfully blue-shifted as much as 70 nm from the previously reported green emitter **Py-TPI** by replacing the thiophene bridge with a benzene bridge. A simple blue OLED with only two organic layers of **Py-BPI** and BPhen demonstrated high efficiencies of 3.93 cd/A and 3.20 lm/W and little current efficiency roll-off even at a high current density of 300 mA/cm^2.

Acknowledgments

This work was supported by National Natural Science Foundation of China (No. 51273108 and No. 91027041), the National Basic Research Program of China (No. 2013CB834803) and the Research Grants Council of the Hong Kong Special Administrative Region, China (Project No. T23-713/11).

Appendix A. Supplementary data

Supplementary data related to this article can be found at http://dx.doi.org/10.1016/j.dyepig.2013.01.022.

References

[1] Gao ZQ, Mi BX, Chen CH, Cheah KW, Cheng YK, Wen WS. Appl Phys Lett 2007;90:123506.
[2] Su SJ, Cai C, Kido JJ. Chem Mater 2011;23:274.
[3] Anthony JE. Angew Chem Int Ed 2008;47:452.
[4] Shirota Y, Kageyama H. Chem Rev 2007;107:953.
[5] Huang JH, Su JH, Tian H. J Mater Chem 2012;22:10977.
[6] Bevilacqua PC, Kierzek R, Johnson KA, Turner DH. Science 1992;258:1355.
[7] Jia WL, McCormick T, Liu QD, Fukutani H, Motala M, Wang RY, et al. J Mater Chem 2004;14:3344.
[8] Tong QX, Lai SL, Lo MF, Chan MY, Ng TW, Lee ST, et al. Synth Met 2012;162:415.
[9] Lai SL, Tong QX, Chan MY, Ng TW, Lo MF, Ko CC, et al. Org Electron 2011;12:541.
[10] Figueira-Duarte TM, Klaus M. Chem Rev 2011;111:7260.
[11] Zhang Y, Lai SL, Tong QX, Chan MY, Ng TW, Wen ZC, et al. J Mater.Chem 2011;21:8206.
[12] Zhang Y, Lai SL, Tong QX, Lo MF, Ng TW, Chan MY, et al. Chem Mater 2012;24:61.
[13] Miyaura N, Suzuki A. Chem Rev 1995;95:2457.
[14] Eaton DF, Houk KN, Iwamura H, Kuzmin MG, Michl J, Tokumaru K. Pure Appl Chem 1988;60:1107.
[15] Naka S, Okada H, Onnagawa H, Tsutsui T. App Phys Lett 2000;76:197.
[16] Hung WY, Ke TH, Lin YT, Wu CC, Hung TH, Chao TC, et al. Appl Phys Lett 2006;88:064102.
[17] Tse SC, Kwok KC, So SK. Appl Phys Lett 2006;89:262102.
[18] Huang J, Sun N, Yang J, Tang RL, Li QQ, Ma DG, et al. J Mater Chem. DOI: 10.1039/c2jm31855e.
[19] Yu DG, Zhao FC, Zhang Z, Han CM, Xu H, Li J, et al. Chem Commun 2012;48:6157.
[20] Thangthong AM, Prachumrak N, Tarsang R, Keawin T, Jungsuttiwong S, Sudyoadsuk T, et al. J Mater Chem 2012;22:6869.
[21] Shimizu M, Mochida K, Asai Y, Yamatani A, Kaki R, Hiyama T, et al. J Mater Chem 2012;22:4337.
[22] Tang S, Li WJ, Shen FJ, Liu DD, Yang B, Ma YG. J Mater Chem 2012;22:4401.
[23] Lee MT, Chen HH, Liao CH, Tsai CH, Chen CH. Appl Phys Lett 2004;85:3301.
[24] Tao S, Xu S, Zhang X. Chem Phys Lett 2006;429:622.
[25] Park JW, Kim YH, Jung SY, Byeon KN, Jang SH, Lee SK, et al. Thin Solid Films 2008;516:8381.
[26] Park JY, Jung SY, Lee JY, Baek YG. Thin Solid Films 2008;516:2917.
[27] Tang C, Liu F, Xia YJ, Lin J, Xie LH, Zhong GY, et al. Org Electron 2006;7:155.
[28] Tao S, Lee CS, Lee ST. Appl Phys Lett 2007;91:013507.
[29] Kuo CJ, Li TY, Lien CC, Liu CH, Wu FI, Huang MJ. J Mater Chem 2009;19:1865.
[30] Lee SJ, Park JS, Yoon KJ, Kim YI, Jin SH, Kang SK, et al. Adv Funct Mater 2008;18:3922.
[31] Chien CH, Chen CK, Hsu FM, Shu CF, Chou PT, Lai CH. Adv Funct Mater 2009;19:560.
[32] Park JK, Lee KH, Kang S, Lee JY, Park JS, Seo JH, et al. Org Electron 2010;11:905.